Neutron scattering study of spin waves and exchange interactions in ferromagnetic EuS

H. G. Bohn and W. Zinn

Institut für Festkörperforschung, Kernforschungsanlage Jülich,
Jülich, Federal Republic of Germany

B. Dorner and A. Kollmar

Institut Laue-Langevin, Grenoble, France
(Received 27 June 1980)

From inelastic neutron scattering the strongly anisotropic spin-wave dispersion curves of a ^{153}EuS single crystalline sample have been measured at 1.3 K for the main symmetry directions $\langle 100 \rangle$, $\langle 110 \rangle$, and $\langle 111 \rangle$ over the entire first Brillouin zone. Least-squares fits to the Holstein-Primakoff spin-wave theory yield the isotropic exchange energy constants, J_i, up to fifth nearest neighbors ($i = 5$) as follows: $J_1/k_B = 0.221 \pm 0.003$ K, $J_2/k_B = -0.100 \pm 0.004$ K, $J_3/k_B = 0.006 \pm 0.002$ K, $J_4/k_B = -0.007 \pm 0.002$ K, $J_5/k_B = -0.004 \pm 0.002$ K which correspond to a paramagnetic Curie temperature of $\Theta_P = 21.1 \pm 0.2$ K. The results confirm previous assumptions that the range of the J_i is essentially limited to next nearest neighbors, and thus agree fairly well with most of the previous experimental results on J_1 and J_2. The temperature dependence of the J_i disagrees with the predictions of the spin-wave renormalization theory.

I. INTRODUCTION

The ferromagnetic insulators EuO and EuS, which crystallize in cubic rocksalt structure, are considered the best examples for the Heisenberg model of ferromagnetism. For comparison between theory and experiment a large body of experimental and theoretical results has been accumulated and reviewed extensively already (see, e.g., Ref. 1 and references therein). In all these studies the exchange interaction parameters J_1 to the 12 nearest and J_2 to the 6 next nearest neighbors have been determined on the basis of an *ad hoc* assumption, namely, that their range is constricted to next-nearest-neighbor distances. There were, however, theoretical arguments and experimental results, which indicated that in the Eu chalcogenides the exchange interactions may range to more distant neighbors.[2,3] EuS is of particular interest because it orders ferromagnetically despite its competing interactions $J_1 > 0$ and $J_2 < 0$ and of its relatively strong dipolar interactions, which are not negligible here in comparison to the exchange interaction.

Recently considerable theoretical and experimental interests have been focused on the $Eu_xSr_{1-x}S$ dilution series. Its unique magnetic behavior and phase diagram was shown to be also due to this competing exchange interactions.[4] The detailed knowledge of the magnitude, sign, and range of the exchange interactions turned out to be the key information for the understanding of the phase diagram and magnetic behavior of this model system for the diluted Heisenberg ferromagnet.

Inelastic neutron scattering is known to be the best source for information on magnetic interactions between neighboring atoms. With Eu compounds, however, the measurement of spin-wave dispersion (SWD) curves turned out to be extremely difficult, because of the unusually high neutron absorption cross section of europium. A previous neutron scattering experiment could be performed only by using a thin powder sample of EuS highly enriched with the ^{153}Eu isotope. From these powder results the above-mentioned *ad hoc* assumption on the range of the exchange interactions, however, could not be removed. This requires the determination of the magnitude and sign of a sufficient large number of individual exchange parameters J_i by measuring the anisotropy and the detailed behavior of the SWD branches of single crystals, in particular, near to the edge of the first Brillouin zone. In fact, just this information is averaged out in the case of polycrystalline EuS samples. Here we report on a first detailed neutron scattering study of all SWD branches using an appropriate single crystalline sample of ^{153}EuS.

II. THEORETICAL MODEL

As is well known the $4f$ electrons of the divalent Eu^{+2} ions are highly localized, thus establishing an $^8S_{7/2}$ ground state with a spin-only magnetic moment

of $7\mu_B$. Then the spin dependent part of the Coulomb interaction between two atomic configurations, having localized spins S_m and S_n, at lattice sites $\vec{R}_m$ and $\vec{R}_n$, respectively, is given by the Heisenberg operator

$$\hat{\mathcal{H}}_{nm} = -2J_{nm}S_n S_m \ .\tag{1}$$

J_{nm} is the related exchange energy parameter. In EuS, because of the relatively weak exchange interactions and the low Curie temperature, $T_c = 16.6$ K, the dipolar interactions of about 2 K in temperature units have to be taken into account too. The Holstein-Primakoff spin-wave theory rather than the original Bloch theory has then to be applied. Neglecting the spin-wave interactions and converting the dipolar sums into surface integrals one arrives at the following formula for the spin-wave energies[5]:

$$\hbar\omega_{\vec{q}} = [\,(g\mu_B B_i + E_{ex})(g\mu_B B_i + E_{ex}$$
$$+ g\mu_B\mu_0 M \sin^2\theta_{\vec{q}})\,]^{1/2} \ ,\tag{2}$$

where $B_i = B_0 - N_D\mu_0 M$ denotes the internal field, which is the applied field, B_0, reduced by the demagnetizing field $-N_D\mu_0 M$. M is the magnetization and N_D the demagnetizing factor depending on sample geometry only. $\theta_{\vec{q}}$ is the angle between the wave vector $\vec{q}$ and the direction of magnetization.

The spin-wave energies of a purely exchange-coupled system, E_{ex}, are given by[6]:

$$E_{ex} = 2S\sum_{\vec{q}}[J(0) - J(\vec{q})] \ ,\tag{3}$$

where

$$J(\vec{q}) = \sum_{\vec{\tau}} J_{nm} e^{i\vec{q}\cdot\vec{\tau}} \ .\tag{4}$$

For S-state ions as Eu^{2+} in the cubic EuS crystal lattice the exchange interactions are expected to be isotropic. In fact, the measured crystalline anisotropy field is of the order of 4 mT only.[7] Equation (4) then can be written in the form

$$J(\vec{q}) = \sum_i J_i \sum_{n=1}^{z_i} e^{i\vec{q}\cdot\vec{\tau}_n} \ ,\tag{4a}$$

where J_i describes the isotropic exchange interactions of an Eu^{2+} ion with its z_i neighbors of the ith neighbor shell. The lattice sums can be evaluated easily for fcc lattices and, depending on the range of interactions, $J(\vec{q})$ then reduces to only a few terms.

Thus, if the internal field and the magnetization of the sample are known, the measurement of the SWD branches on a single crystalline sample will yield the exchange parameters $J_i(i \leq r)$.

III. EXPERIMENTAL CONDITIONS

Europium consists of two isotopes ^{151}Eu and ^{153}Eu with natural abundances of 48% and 52%, respectively. Because of the extremely high neutron absorption cross section of the ^{151}Eu isotope for our inelastic neutron scattering experiment EuS single crystals were grown from the melt of EuS powder, which was enriched to 99.2% with ^{153}Eu. The crystals were cleaved into the platelets of 0.3-mm thickness or less. The faces of these platelets were crystallographic (100) planes and a $\langle 010\rangle$ axis within the plane could easily be identified. The oriented platelets of a few mm^2 size were glued on an aluminum substrate and finally realized a crystallographic (100) plane of 3×5 cm^2 in size. The total weight of the sample was 2.3 g. The orientation of the platelets was checked by x-ray and neutron-diffraction techniques. The remaining misorientation of the described mosaic arrangement was found to be less than $3°$. The Curie temperature of the sample was determined from hysteresis measurements to be $T_c = 16.6$ K,[8] which is the value for stoichiometric EuS.

The neutron scattering experiments were performed at the high-flux reactor of the Institut Laue-Langevin, Grenoble using the IN2 triple axis spectrometer. The spectra were recorded in the constant q mode near the forward direction. Most of the measurements were made with incoming neutron energies of 13.7 meV; only for the smallest q values and the weakest spin-wave energies, in particular, of the $\langle 111\rangle$ branch initial energies of 6.7 and 4.9 meV were also used for better energy resolution. Appropriate filters were placed in the primary beam to avoid higher-order contributions. The SWD has been investigated at the temperatures 1.3, 2.2, and 4.2 K. A few spin-wave spectra were also measured up to higher temperatures close to the Curie temperature. Temperatures below 4.2 K were determined by means of the ^{4}He vapor pressure, while for those above 4.2 K a calibrated carbon resistor was used.

In order to obtain well-defined magnetization conditions, two SmCo$_5$ permanent magnets were mounted above and below the sample. An external field of about 0.08 T was thus applied in the plane of the EuS platelets where it fairly exceeded the demagnetizing field $-N_D\mu_0 M$ (the saturation magnetization at $T = 0$ K is $\mu_0 M = 1.53$ T) making $B_i \approx 0$.

Thus the platelets could be kept homogeneously magnetized in a direction perpendicular to the scattering vector ($\sin\theta = 1$).

IV. RESULTS AND DISCUSSION

Typical spectra measured for spin waves propagating in the $\langle 110\rangle$ direction are shown in Fig. 1. For the purpose of this study outlined above we were interested only in the position of the maximum of the magnon lines. These were deduced from a least-squares fit of the data to two Gaussian lines: One of these accounts for the elastically scattered neutrons

as determined using the width and position of a vanadium spectrum, while the second one describes the neutrons scattered inelastically on spin waves. The spectrometer resolution function,[9] the thermal detailed balance factor, and the overall background were properly taken into account. The solid lines in Fig. 1 represent the best fit to the data. For $q = 6.0$ nm^{-1}, where the spin-wave line appears only in the tail of the elastic line, the contribution of the inelastic magnetic scattering is indicated by the dashed line.

The width of the magnon lines at 1.3 K is due to the spectrometer resolution only. For comparison the spectrum obtained with a polycrystalline sample at $q = 10.4$ nm^{-1} is also plotted in Fig. 1. It reveals the substantial powder broadening which exists especially near to the boundary of the first Brillouin zone. Due to this large anisotropy of the SWD branches the position and width of the magnon lines can be determined in detail and with high accuracy only by using single-crystal samples.

The experimental data are summarized in numeric form in Table I. With systematic errors of the measurements taken into account we estimate the uncertainty of the magnon energies to ± 0.02 THz while the error in determining an individual inelastic peak is smaller typically by an order of magnitude.

For the geometrical and magnetic conditions described above the spin-wave dispersion relation of Eq. (2) then reduces to

$$\hbar\omega_{\vec{q}} = \{E_{ex}[E_{ex} + g\mu_B\mu_0 M(T)]\}^{1/2} . \qquad (5)$$

The spin-wave spectra have been analyzed by taking into account exchange constants J_i up to the sixth
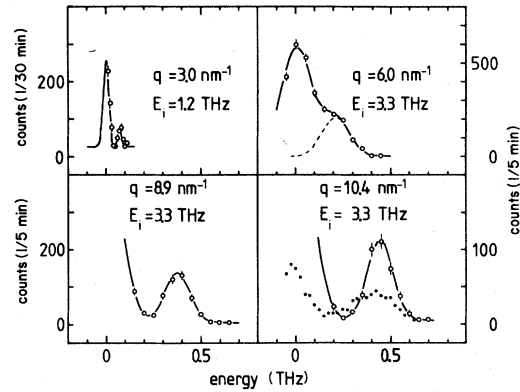

FIG. 1. Neutron spectra for inelastic scattering on spin waves in single crystalline ^{153}EuS. The wave vector $\vec{q}$ is directed along the crystallographic $\langle 110 \rangle$ direction. For comparison a spectrum obtained with a powder sample at $q = 10.4$ nm is also shown ($\bullet$). The solid line is the best fit to the measured points. The dashed line indicates the contribution due to the inelastic scattering on magnons.

nearest neighbors ($i = 6$). The J_i have been determined from the spectra at 1.3 K, where the normalized magnetization deviates by only 5×10^{-3} from its saturation value (using $M_0 = 1.53$ T and including the zero-point motion due to the dipolar interactions). In this way spin-wave interactions which would lead to a renormalization of the exchange parameters[10] can be neglected.

In Fig. 2 the SWD curves in the main symmetry directions, $\langle 100 \rangle$, $\langle 110 \rangle$, and $\langle 111 \rangle$, as measured at

TABLE I. Magnon energies in EuS for the three main symmetry directions. Taking into account systematic errors, the accuracy of each energy is ± 0.02 THz.

$\langle 100 \rangle$		$\langle 110 \rangle$		$\langle 111 \rangle$	
q (nm^{-1})	E (THz)	q (nm^{-1})	E (THz)	q (nm^{-1})	E (THz)
2.64	0.050	2.99	0.071	3.66	0.087
3.17	0.073	4.48	0.137	5.49	0.156
4.23	0.123	5.98	0.213	7.32	0.211
5.28	0.225	5.98	0.177	9.15	0.236
5.28	0.226	7.47	0.280		
6.34	0.319	8.96	0.359		
6.87	0.360	9.86	0.395		
7.40	0.412	10.46	0.430		
7.92	0.450	11.21	0.459		
8.45	0.491	11.21	0.461		
8.98	0.519	11.95	0.484		
9.51	0.539	12.70	0.507		
10.04	0.557	13.45	0.521		
10.57	0.554	14.19	0.535		
		14.94	0.532		

$J_1/k = 0.221$ K
$J_2/k = -0.100$ K
$J_3/k = 0.006$ K
$J_4/k = -0.007$ K
$J_5/k = -0.004$ K

EuS

⟨100⟩ ⟨110⟩ ⟨111⟩

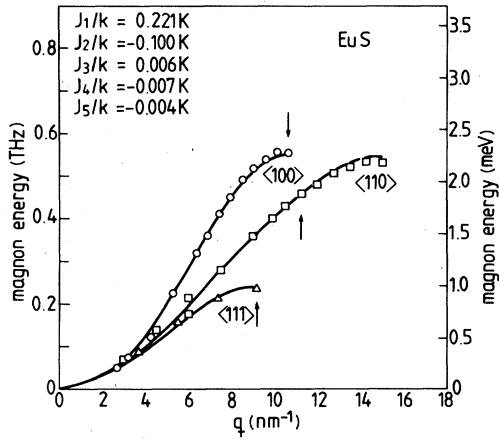magnon energy (THz)

magnon energy (meV)

q (nm^{-1})

FIG. 2. Spin-wave dispersion in a ^{153}EuS single crystal at 1.3 K. The solid lines represent the best fit using up to fifth neighbors exchange interactions. The arrows indicate the boundary of the first Brillouin zone in the different symmetry directions. Including systematic errors of the measurement an error bar of ± 0.02 THz is given to each point.

the temperature 1.3 K are plotted. The arrows indicate the boundary of the 1st Brillouin zone in these directions. By fitting the experimental data to Eq. (5) using the exchange constants $J_1, \ldots, J_6$ as parameters of the fit the values summarized in Table II were obtained. Apparently, only J_1 and J_2 are of substantial magnitude, whereas the exchange constants $J_3, \ldots, J_6$ are smaller by more than an order of magnitude and, hence, in the range of the experi-

mental errors already. We would like to emphasize, however, that $J_3, \ldots, J_6$ are comparable with the attributed dipolar interactions of these neighbors, which are listed in the last line of Table II, too. Thus, they are expected to be important, in particular, for discussions of very diluted $Eu_xSr_{1-x}S$ systems.[11]

The solid lines in Fig. 2 represent the best fits of the dispersion curves derived with the $J_{1,2}$ values given in line 5 of Table II and including $J_{3,4,5}$ as small corrections. We have chosen these values, since according to column 8 of Table II the sum of squares of the deviations divided by the degrees of freedom (i.e., the number of experimental points minus the number of parameters) does not further decrease with J_6 included. Also, the value of J_6 is smaller than the statistical uncertainty. These results fortunately prove that in EuS the exchange interactions in fact reach to nearest and next nearest neighbors only, as it has been assumed ad hoc only in all experiments before. The ratio of J_1/J_2, which is of particular importance for the understanding of the magnetic phase diagram of the $Eu_xSr_{1-x}S$ system is found to be $J_1/J_2 = -2.2 \pm 0.1$ which is, in fact, close to the value -2 used in most of the recent theoretical work.[12]

Our results agree well with the exchange parameters determined from the neutron scattering experiment with a polycrystalline ^{153}EuS sample as mentioned before.[10] This is not surprising now, since our single crystal results confirmed that NN and NNN interactions only are of substantial magnitude as it has been introduced ad hoc in this earlier neutron scatter-

TABLE II. Results of the least-squares fits of the SWD curves for different numbers of exchange constants N. In the last column the sum of squares of the deviations, χ^2, divided by $M - N$ is given, where $M = 33$ is the number of experimental points. $W_{dip} = \mu_0/4\pi\mu^2/r^3$ is a measure for the dipolar energy.

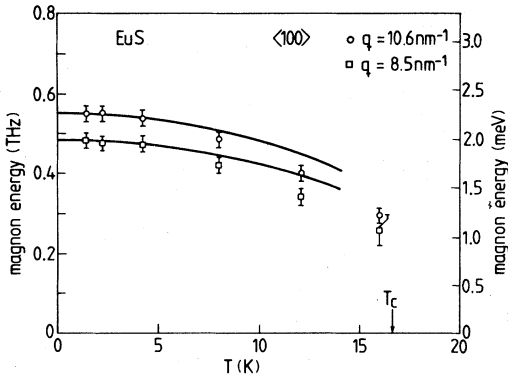| N	J_1/k_B (K)	J_2/k_B (K)	J_3/k_B (K)	J_4/k_B (K)	J_5/k_B (K)	J_6/k_B (K)	$10^4 \dfrac{\chi^2}{M-N}$
2	0.224 ± 0.002	-0.111 ± 0.004					1.61
3	0.219 ± 0.003	-0.113 ± 0.004	0.002 ± 0.002				1.55
4	0.217 ± 0.003	-0.105 ± 0.005	0.005 ± 0.002	-0.007 ± 0.002			1.22
5	0.221 ± 0.003	-0.100 ± 0.004	0.006 ± 0.002	-0.007 ± 0.002	-0.004 ± 0.002		0.98
6	0.220 ± 0.003	-0.099 ± 0.005	0.007 ± 0.002	-0.007 ± 0.002	-0.005 ± 0.002	-0.002 ± 0.003	0.99
W_{dip}/k_B (K)	0.41	0.13	0.07	0.05	0.03	0.03	

FIG. 3. Temperature dependence of the spin-wave energies in ^{153}EuS for two q values near the boundary of the first Brillouin zone in the $\langle 100 \rangle$ direction. The solid lines represent calculations based on spin-wave renormalization theory using the exchange constants given in Fig. 2.
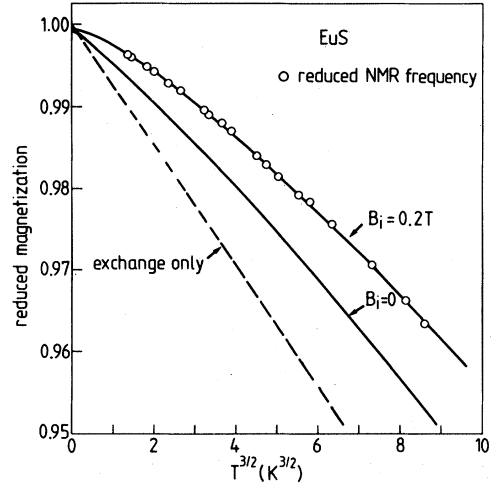

FIG. 4. Temperature dependence of the normalized zero-field NMR frequency, f/f_0 ($f_0 = 152.222$ MHz). The experimental points were taken from Ref. 16. The solid lines represent the normalized magnetization, M/M_0, for $B_i = 0$ and $B_i = 0.2$ T calculated from spin-wave theory using the exchange constants given in Fig. 2 and including the dipolar contributions. The dashed line results for $B_i = 0$, if pure exchange coupling is taken into account.

ing work, too. Even then, in view of the considerable powder broadening, apparent from both our spectra shown in Fig. 1, and the anisotropy of the SWD curves shown in Fig. 2, the good agreement of the $J_{1,2}$ results deduced from both experiments must be called remarkable.

V. SPIN-WAVE RENORMALIZATION

Next, we would like to discuss the temperature dependence of the measured SWD curves as shown in Fig. 3 for two q values near the edge of the first Brillouin zone, in the $\langle 100 \rangle$ direction.

The solid lines have been calculated using the spin-wave renormalization theory developed by Dyson[13] and by Keffer and Loudon,[14] together with the exchange constants as determined from our low-temperature SWD results. Obviously, the theory describes our data for EuS adequately for $T/T_c < 0.25$ only. This is in contrast to the case of EuO, where it was found to hold up to $T/T_c < 0.9$.[15] This is supposed to be due to the relatively large dipolar contribution in EuS. The clarification must await the forthcoming more detailed study of the temperature dependence of the spin-wave spectra.

VI. COMPARISON WITH MAGNETIZATION STUDIES

The temperature dependence of the spontaneous magnetization can be precisely determined from the zero-field NMR frequency, f, since

$$\frac{M(T)}{M_0} = \frac{f(T)}{f_0} \ . \tag{6}$$

The relative error in this experiment is 10^{-4}.[16] Figure 4 shows the temperature dependence of the nor-

malized NMR frequencies which were taken from Ref. 16 and using $f_0 = 152.222$ MHz. The solid lines represent the reduced spontaneous magnetization as calculated in the spin-wave regime using the Holstein-Primakoff dispersion law [Eq. (2)] and the exchange constants determined from our low-temperature (SWD) curves for $B_i = 0$ and $B_i = 0.2$ T, respectively. The calculations were carried out by exact numerical integration over the first Brillouin zone, and considering additionally for the renormalization of the exchange parameters at higher temperatures. It should be noted that at $T = 0$ K the magnetization does not fully reach its saturation value M_0. This is due to the zero-point motion which results from the dipolar contributions.[5] The dashed line results for the purely exchange-coupled system with the same exchange parameters as above. From the least-squares fit of the reduced magnetization curve as deduced from the NMR frequencies the values for the frequency and the effective internal magnetic field B_i have been determined to $f_0 = 152.222$ MHz and $B_i = 0.2$ T, respectively. The origin of the non-zero internal field value obtained here again as in all previous zero external field NMR studies on EuS,[17, 18] is uncertain. Internal stray fields to be expected due to the particular domain structure of EuS (see, e.g., Ref. 19) and anisotropy fields are found to be smaller by more than an order of magnitude by magnetization studies on the same single crystalline spheres[20] used in the NMR work.

Hence, it must be left as an open question whether the final internal field parameter does not reflect only limitations in the applied theoretical model.

In the neutron scattering experiment the thin sample has been magnetized homogeneously in the sample plane and, hence, $B_i \approx 0$ was well determined in this case. On the other hand, in the neutron scattering result of the SWD curve on Fig. 2 even a value $B_i = 0.2$ T would cause an energy gap of 5×10^{-3} THz only, which could hardly be drawn in Fig. 2 and which was shown to influence the determination of the exchange parameters J_i by far less than the error limits given in Table II. In contrast, the NMR results are most sensitive to details of the SWD curve at very small q values, and to the proper inclusion of the dipolar interactions in the theoretical model for this regime.

It should be mentioned finally, that the paramagnetic Curie temperature, $\Theta_P = \frac{2}{3} S (S+1) \sum_i z_i J_i / k_B$ according to the J_i/k_B results given in Table II is $\Theta_P = 21.1 \pm 0.2$ K. This is in fair agreement with the value of 21.8 K expected theoretically from the ratio $T_c / \Theta_P = 0.76$.[21]

VII. SUMMARY

We have shown by these inelastic neutron scattering experiments on single crystalline ^{153}EuS, that the SWD curves in the $\langle 100 \rangle$, $\langle 110 \rangle$, and $\langle 111 \rangle$ symmetry directions are highly anisotropic. They can be explained by the isotropic positive NN, and negative NNN exchange interaction parameters $J_1/k_B = 0.220$ K and $J_2 = -0.45 J_1$, respectively, while the more distant neighbor interactions $J_{3,4,5,6}$ decrease to a few percent of J_2 only. Hence, they are still smaller than the dipolar interactions, which therefore have to be taken into account properly in the data analysis.

Using the Holstein-Primakoff spin-wave theory both the SWD curves and the spontaneous magnetization curves as deduced from zero-field NMR measurements can be described accurately by the same set of exchange parameters $J_{1,2,3,4,5}$. For explaining the zero-field NMR result an internal field of $B_i = 0.2$ T had to be taken into account. The origin of this field is uncertain.

The measured temperature dependence of the spin-wave energies is shown to be in disagreement with the spin-wave renormalization theories of Dyson, Keffer, and Loudon.

[1]W. Zinn, J. Magn. Magn. Mater. **3**, 23 (1976).

[2]G. A. Sawatzky, W. Geertsma, and C. Haas, J. Magn. Magn. Mater. **3**, 37 (1976).

[3]G. Crecelius, H. Maletta, H. Pink, and W. Zinn, J. Magn. Magn. Mater. **5**, 150 (1977).

[4]H. Maletta, J. Phys. (Paris) **41**, C5-115 (1980).

[5]T. Holstein and H. Primakoff, Phys. Rev. **58**, 1098 (1940); F. Keffer, *Encyclopedia of Physics* (Springer-Verlag, Berlin, 1966), Vol. XVIII/2, p. 49.

[6]Reference 5, p. 44.

[7]G. E. Everett and R. A. Ketcham, J. Phys. (Paris) **32**, C1-545 (1971).

[8]B. Saftić (private communication).

[9]B. Dorner, Acta Crystallogr. Sect. A **28**, 319 (1972).

[10]L. Passell, O. W. Dietrich, and J. Als-Nielsen, Phys. Rev. B **11**, 4897 (1976); see also Refs. 13 and 14.

[11]J. Kötzler and G. Eiselt, J. Phys. C (1980) (in press).

[12]K. Binder, W. Kinzel, and D. Stauffer, Z. Phys. B **36**, 161

(1979); K. Binder, W. Kinzel, H. Maletta, and D. Stauffer, J. Magn. Magn. Mater. **15—18**, 189 (1980).

[13]F. J. Dyson, Phys. Rev. **102**, 1217 (1956); **102**, 1230 (1956).

[14]F. Keffer and R. Loudon, J. App. Phys. Suppl. **32**, 25 (1961).

[15]O. W. Dietrich, J. Als-Nielsen, and L. Passell, Phys. Rev. B **14**, 4923 (1976).

[16]M. Neusser, H. Lütgemeier, and W. Zinn, J. Magn. Magn. Mater. **4**, 42 (1977).

[17]S. H. Charap and E. L. Boyd, Phys. Rev. **133**, A811 (1964).

[18]O. W. Dietrich, A. J. Henderson, and H. Meyer, Phys. Rev. B **12**, 2844 (1975).

[19]P. Tischer, IEEE Trans. Magn. **9**, 9 (1973).

[20]U. Köbler (private communication).

[21]U. Köbler and K. Binder, J. Magn. Magn. Mater. **15—18**, 313 (1980).